COMMUNICATION

Check for updates

Molecular recognition and adsorptive separation of *m*-xylene by trianglimine crystals†

Avishek Dey,[a] Santanu Chand,[a] Munmun Ghosh,[a] Monerah Altamimy,[a] Bholanath Maity,[b] Prashant M. Bhatt, [iD][c] Imtiyaz Ahmad Bhat,[a] Luigi Cavallo, [iD][b] Mohammed Eddaoudi [iD][c] and Niveen M. Khashab [iD] *[a]

The separation of xylene isomers is one of the most challenging tasks in the petrochemical industry. Herein, we developed an efficient adsorptive molecular sieving strategy using crystalline trianglimine macrocycle (1) to separate the elusive *m*-xylene isomer from an equimolar xylenes mixture with over 91% purity. The selectivity is attributed to the capture of the preferred guest with size/shape selectivity and C−H⋯π interactions. Moreover, the trianglimine crystals are readily recyclable due to the reversible transformation between the guest-free and guest-loaded structures.

The energy intensive separation and purification of petrochemical isomers currently consumes 10–15% of the world's total energy production. Separation of C₈ aromatics, *o*-xylene (OX), *p*-xylene (PX), *m*-xylene (MX) and ethylbenzene (EB), is considered as one of the 'seven chemical separations that will change the world.'[1] Xylenes are obtained from crude oil by catalytic reforming and pyrolysis of gasoline. Each of the isomers is an important building block in the production of polymer fibers, films, plasticizers, resins, *etc.*[2–4] Separation of MX from a mixture of OX/MX/PX is highly demanding as these isomers have overlapping physical properties.[5,6] Chromatographic separation and other processes such as enclathration can be considered as energy saving options however, they are labor and time intensive.[7–10]

Employing porous materials especially for C₈ aromatics separation has recently gained a lot of attention.[11] Zeolites and metal organic frameworks (MOFs) have shown effective industrial separation of OX and PX but more efforts are needed to obtain desired separation performance.[12–17] Porous organic cages, with complementary geometry suitable for specific host molecules, were also employed for energy-demanding separations but showed modest performance for the separation of isomers.[18–20] Nonporous adaptive crystals (NACs) based on macrocyclic building blocks such as pillar[6]arene have been successfully utilized for the separation of *p*-xylene and other isomer from their mixtures in the vapor phase.[4,21,22] Nonetheless, pillar[6]arene crystals can work only *via* vapor-based adsorption as they are soluble in xylenes, which dramatically limits the possibility for their industrial translation. In this context, our group has recently reported the selective separation of OX and PX by CB[7] and crystalline azo cages, respectively.[6,23] Interestingly, separation of the MX isomer has so far been illusive as host–guest interactions using the molecular sieving approach has mainly preferred PX and OX isomers.

Trianglimine macrocycles have emerged as a novel class of intrinsically porous molecular hosts that can be specifically tailored for selective separations.[24] Herein, we report that macrocycle 1 can be used as a host for the encapsulation and separation of MX from the xylene isomers both in the liquid and vapor phases through shape selective crystallization and the adsorption based approach (Fig. 1a and Fig. S1, ESI†). To the best of our knowledge, no systematic investigation was reported thus far on the use of organic macrocycles for the separation of MX from xylene isomers by the molecular sieving approach.

The synthesis and crystal structure of the macrocyclic host 1 have already been reported by our group.[25,26] It crystallizes in a monoclinic system, chiral space group P2₁ and the asymmetric unit contains one unit of trianglimine and disordered solvent molecules (Table S1, ESI†). The structural analysis also revealed that two trianglimines are nearly perpendicular and stacked in

[a] Smart Hybrid Materials (SHMs) Laboratory, Advanced Membranes and Porous Materials Center, King Abdullah University of Science and Technology (KAUST), Thuwal 23955-6900, Kingdom of Saudi Arabia.
E-mail: niveen.khashab@kaust.edu.sa

[b] King Abdullah University of Science and Technology (KAUST), KAUST Catalysis Center (KCC), Thuwal 23955-6900, Kingdom of Saudi Arabia

[c] Functional Materials Design, Discovery and Development Research Group, Advanced Membranes and Porous Materials Center, Division of Physical Sciences and Engineering, King Abdullah University of Science and Technology (KAUST), Thuwal 23955-6900, Kingdom of Saudi Arabia
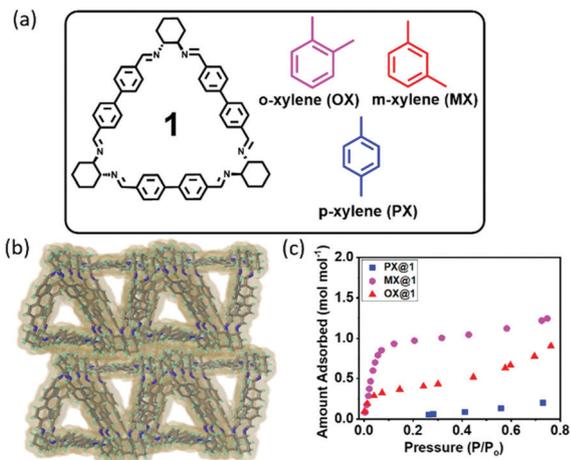
Fig. 1 (a) Chemical structure of macrocycle **1** and the three xylene isomers. (b) Packing of the activated structure **1A**. (c) Vapor adsorption isotherm of **1** at 298 K.
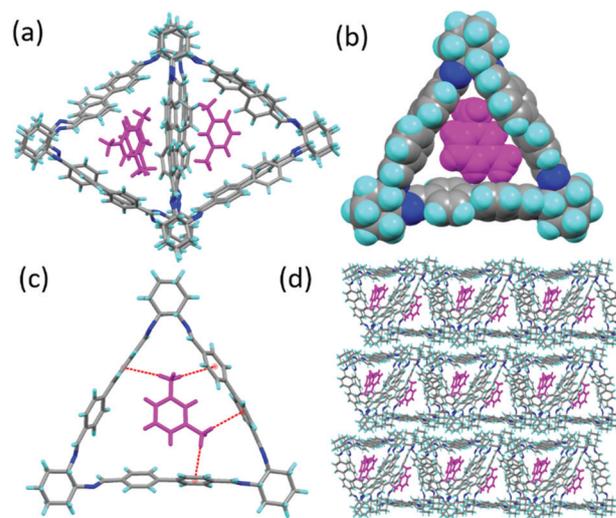

Fig. 2 Description of the single crystal structure of **MX@1**: (a) how the MX intercalates with host. (b) Space filling model shows how MX fits in the intrinsic cavity of the host. (c) Host–guest complex is stabilized by C−H···π interaction. (d) Packing shows that layered structure with connecting channels occupying MX. (Color code: C, grey; N, blue; H, cyan; MX, magenta).

layered structure with head–tail fashion along the b axis. The apohost (**1A**) obtained from activation of **1** (70 °C for 24 h under high vacuum), is designed with an intrinsic cavity of 12 Å that can be ideal for the xylene isomers (Fig. 1a and Table S2, ESI†). Crystal structure analysis revealed the same crystal system and similar type of layered structured packing even after removal of the solvent molecules from the channels (Fig. 1b and Fig. S2 and S3, ESI†). The activated structure retains its imprinted cavity after solvent removal to re-adsorb xylene. In an attempt to investigate the porosity of **1** towards guest molecules, single component vapor adsorption experiments were recorded at 298 K for each of the commercially pure xylene isomers (Fig. 1c). It was found that MX vapor was adsorbed most rapidly by the host at low relative pressure ($P/P_0 < 0.1$), and adsorbed 1.076 mol^{-1} of MX. This can be attributed to the strong adsorbent–adsorbate interactions in **MX@1**. In contrast, adsorption of OX and PX was notably negligible at low relative pressure ($P/P_0 < 0.1$) and it gradually went to saturation at high pressure in case of OX vapor. It is worth noting that the host did not adsorb PX vapor even at high relative pressure. This indicates that preexisting pores of **1A** are preferentially stabilized when they are occupied with MX vapor at low relative pressure ($P/P_0 < 0.1$) compared to other isomers. The results indicate that **1** can selectively adsorb MX at low pressure and the selectivity order is MX ≫ OX ≫ PX.

To better understand this adsorption behavior, a detailed study of the host–guest interactions was performed. Attempts to crystallize **1** in dichloromethane (DCM)/acetonitrile (ACN)/MX (2 : 1 : 1) by slow evaporation resulted in the formation of block prism shaped single crystals of **MX@1** after 2 days (Table S3, ESI†). SCXRD analysis revealed that it crystallizes in a triclinic crystal system, chiral $P1$ space group and the asymmetric unit contains four units each of **1** and **MX** (Fig. 2a). Two trianglimine units are overlapped with each other and they are perpendicular to other overlapped two trianglimine units when viewed along the crystallographic a axis (Fig. S4, ESI†). MX best fits in the intrinsic triangular cavity of **1** with respect to

orientation and packing. The space filling model also represents that it is fits the best in the interior cavity (Fig. 2b). This is driven by C−H···π interactions (2.764 Å) between MX and one of the aromatic rings of the macrocycle (Fig. 2c). The trianglimine units are connected to one another by weak π···π interactions (4.397 Å) between the aromatic rings which promotes them to form the layered structure and perpendicular arrangements (Fig. S4, ESI†). The triangular macrocycle molecules, when assembled in a window to window packing mode, also form a layered structure which contributes to the formation of one-dimensional triangular channels where MX gets entrapped in the internal cavity of the aligned macrocycles along the crystallographic a axis (Fig. 2d). The guest occupancy was confirmed using residual electron density analysis by the PLATON SQUEEZE.[27,28]

The efforts to get single crystals from OX were proved to be abortive; however, an organogel was obtained with DCM/ethyl acetate/OX (1 : 1 : 1 v/v). Moreover, the single crystal obtained with PX was found to contain only the trianglimine crystals (Fig. 3). This indicates that macrocycle **1** is selective towards the MX isomer. The pillars of trianglimines can cause some distortions which consequently influences the size of the internal cavity; and hence, PX and OX have a chance to be out of plane of the intrinsic cavity, as suggested by DFT calculations. Thermogravimetric analysis (TGA) also confirmed the 1 : 1 host : guest ratio of **1** and MX (Fig. S5, ESI†). Furthermore, powder X-ray diffraction (PXRD) pattern of **MX@1** was well matched with the simulated pattern (Fig. S6a, ESI†). To the best of our knowledge, this is the first report on the separation of MX controlled by the morphology of any organic material, particularly based on crystal shape and phase induction (Fig. 3).
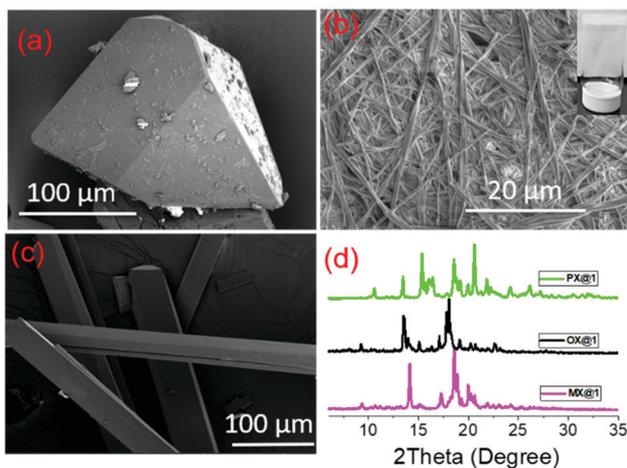
Fig. 3 SEM images of the products formed: (a) crystal obtained from **MX@1**. (b) Organogel obtained from OX and their self-assembly structure. (c) Crystal obtained from PX. (d) PXRD pattern of different forms of xylenes product.

Fig. 4 (a) Solid–vapor sorption of **1** in OX/MX/PX (1:1:1 v/v) xylenes. (b) Time dependent PXRD of **1** to **MX@1** in the presence of OX/MX/PX (1:1:1 v/v) vapor. (c) Relative uptakes of MX after five recycles. (d) Schematic representation of MX release from **MX@1** to **1** upon heating and uptake of MX again from the mixture vapor.

These host–guest interactions and shape/size selectivity prompted us to test whether **1** could discriminate one isomer from a mixture of isomers in the liquid state. Crystallization of **1** in DCM/ACN (2:1) in the presence of a ternary equimolar mixture of o-/m-/p- xylenes (1:1:1 v/v/v) resulted in block prism shaped single crystals after 3 days and SCXRD analysis revealed the selective adsorption of MX over other isomers (Fig. 3 and Fig. S6b, S7, ESI†). The structure was exactly similar to that of **MX@1** crystals, which indicates that this system is also effective for crystallization-based separation with a purity over 99% in the solid–liquid state as verified by GC analysis (Table S4 and Fig. S8, ESI†). The competitive experiments were further tested for binary compositions of xylenes, which also supported the selectivity towards MX (Fig. S6c, ESI†).

Being prompted by the outstanding host–guest properties (as observed in SCXRD), we envisioned the applicability of this system in vapor phase and so we tested the positional sorting effect of xylene isomers. Activated guest free crystals **1** were obtained upon heating **1** at 70 °C for 24 h under high vacuum. After removing the solvent molecules by activation, the crystals exhibited high stability and crystallinity which indicates that the lattice voids are imprinted as verified by SCXRD (Fig. S2, ESI†). ^{1}H NMR spectra, TGA and PXRD experiments were performed to confirm the adsorption selectivity towards MX over other isomers. To reveal the detailed mechanistic pathway for the separation of MX, a time dependent solid–vapor experiment for equimolar mixture containing three xylene isomers (o-/p-/m- 1:1:1 v/v) was performed by **1** to measure the rate of the uptake process. It was found that the uptake of MX in **1A** increased over time and reached a saturation at 24 h; whereas the uptake of OX was competitive over the first three hours and then decreased to negligible quantity. The adsorption of PX was almost negligible throughout the entire period (Fig. 4a). It is possible that MX and OX are both adsorbed in the beginning (kinetically favored), and then when the material is almost
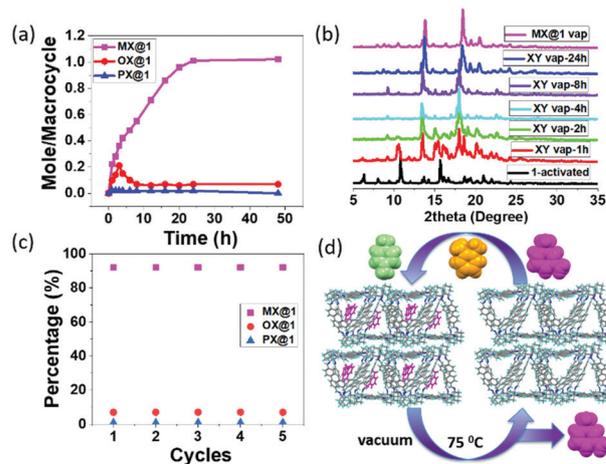
saturated, OX is gradually replaced by MX due to thermodynamic stability. This implies a remarkably selective adsorption of MX from the xylene mixtures through guest capture by the host (Fig. S9–S12, ESI†). Further, PXRD experiments were carried out to monitor the structural transformation of **1** to **MX@1** after exposer to xylene isomers. The PXRD pattern suggests that apohost **1A** transforms to **MX@1** phase after 24 h from exposure to the equimolar mixture of xylene vapors (o-/p-/m- 1:1:1 v/v), while the preferentiality towards the other isomers (OX and PX) were negligible (Fig. 4b, Scheme S1 and Fig. S13a, ESI†). This further confirmed the preference towards MX over PX and OX in the vapor phase. The traditional porous crystalline materials do not change the structures upon guest capture,[29,30] while the "intrinsic porosity" in trianglimine crystals could be induced by preferred guest molecules such as MX. Gas chromatography (GC) showed that **1A** can selectively capture MX over PX and OX in the intrinsic pores of crystalline solids with more than 91% selectivity (Fig. S14, ESI†).

Once we have established that **1A** is selective towards MX, we thought of looking into its performance on commercially relevant samples such as the C_8 aromatic fraction of xylene mixture and ethylbenzene isomer through both liquid and solid–vapor phase. Consistently, it revealed to be selective towards MX from the commercial samples (Fig. S6b and S13b, ESI†). In industrial production processes, the major problems associated with the adsorptive separation is decreasing performance of porous materials over time, because of the instability of the porous framework during heating. To be practically useful, an adsorbent must perform well over multiple cycles without any degradation. Recyclability and reversibility was accordingly verified over five cycles without any loss of selectivity as confirmed by GC (Fig. 4c, d and Fig. S14, S15, ESI†). We then investigated the selectivity of **1** for binary mixtures and again found the formation of **MX@1** from a

mixture of either MX and PX or MX and OX, as confirmed from PXRD (Fig S6c and S16, ESI†).

To estimate the thermochemistry of the formation of **MX@1**, **OX@1** and **PX@1**, density functional theory (DFT) calculations were performed at ωB97xD(SMD)/Def2-TZVP//PBE0-D3/Def2-SVP level of theory. The calculated energy values indicated that the formation of all the **MX@1**, **OX@1** and **PX@1** are exergonic by −24.6, −13.2 and −10.7 kJ mol^{-1} respectively (ΔG_{298}^{Sol}, Scheme S2, ESI†). Therefore, in agreement with the experimental observation, the selectivity order of adsorption is MX > OX > PX. We also performed the distortion-interaction analysis on the electronic structure of **MX@1**, **OX@1** and **PX@1**. This analysis indicated that the ΔE of **MX@1** is in favor of 10.5 kJ mol^{-1} and 13.1 kJ mol^{-1} than that of **OX@1** and **PX@1** respectively (Table S5, ESI†). The highest ΔE values of **MX@1** corresponds to the lowest contribution of ΔE_{dis} of the host fragment **1**, which is unfavored by 17.3 kJ mol^{-1} and 16.6 kJ mol^{-1} relative to that of **OX@1** and **PX@1**. A minor distortion of **1** in **MX@1** with RMSD (root-means-square deviation) of heavy atoms is 0.25 Å, while a clear deviation have been observed in **OX@1** and **PX@1** with RMSD values of 0.66 Å and 0.68 Å respectively. Therefore, the computational studies clearly support that the cavity of **1** is tailored to incorporate the MX molecule, while the adsorption of OX and PX requires a substantial deformation of the macrocycle cavity.

In conclusion, we have demonstrated a new class of intrinsically porous trianglimine macrocycle crystals with shape selective adsorptive molecular sieving of MX from the xylene isomers in both liquid and solid–vapor phase with selectivity over 91% for the multiple times. The present approach relies on the ability of **1** to preferentially capture a guest with "the best fit" and superior host–guest interactions, which was corroborated by DFT calculations. Considering the easy and cheap accessibility, low operating temperature, higher separation efficiency and high recyclability, this material holds a great potential for energy intensive separations through a tailored molecular recognition approach.

Conflicts of interest

There are no conflicts to declare.

Notes and references

1 D. S. Sholl and R. P. Lively, *Nature*, 2016, **532**, 435–437.

2 Y. Yang, P. Bai and X. Guo, *Ind. Eng. Chem. Res.*, 2017, **56**, 14725–14753.

3 N. Sun, S.-Q. Wang, R. Zou, W.-G. Cui, A. Zhang, T. Zhang, Q. Li, Z.-Z. Zhuang, Y.-H. Zhang, J. Xu, M. J. Zaworotko and X.-H. Bu, *Chem. Sci.*, 2019, **10**, 8850–8854.

4 K. Jie, M. Liu, Y. Zhou, M. A. Little, A. Pulido, S. Y. Chong, A. Stephenson, A. R. Hughes, F. Sakakibara, T. Ogoshi, F. Blanc, G. M. Day, F. Huang and A. I. Cooper, *J. Am. Chem. Soc.*, 2018, **140**, 6921–6930.

5 M. Rana, R. B. Reddy, B. B. Rath and U. K. Gautam, *Angew. Chem., Int. Ed.*, 2014, **53**, 13523–13527.

6 G. Zhang, A.-H. Emwas, U. F. S. Hameed, S. T. Arold, P. Yang, A. Chen, J.-F. Xiang and N. M. Khashab, *Chem*, 2020, **6**, 1082–1096.

7 C. J. Egan and R. V. Luthy, *Ind. Eng. Chem.*, 1955, **47**, 250–253.

8 M. O. Daramola, A. J. Burger, M. Pera-Titus, A. Giroir-Fendler, S. Miachon, J. A. Dalmon and L. Lorenzen, *Asia-Pac. J. Chem. Eng.*, 2010, **5**, 815–837.

9 J. Lipkowski, D. D. MacNicol, F. Toda and R. Bishop, *Pergamon, Exeter*, 1996, **6**, 691–714.

10 L. R. Nassimbeni, N. B. Bathori, L. D. Patel, H. Su and E. Weber, *Chem. Commun.*, 2015, **51**, 3627–3629.

11 M. Minceva and A. E. Rodrigues, *AIChE J.*, 2007, **53**, 138–149.

12 D. M. Polyukhov, A. S. Poryvaev, S. A. Gromilov and M. V. Fedin, *Nano Lett.*, 2019, **19**, 6506–6510.

13 M. du Plessis, V. I. Nikolayenko and L. J. Barbour, *J. Am. Chem. Soc.*, 2020, **142**(10), 4529–4533.

14 S. Mukherjee, B. Joarder, B. Manna, A. V. Desai, A. K. Chaudhari and S. K. Ghosh, *Sci. Rep.*, 2014, **4**, 5761.

15 S.-Q. Wang, S. Mukherjee, E. Patyk-Kaźmierczak, S. Darwish, A. Bajpai, Q.-Y. Yang and M. J. Zaworotko, *Angew. Chem., Int. Ed.*, 2019, **58**, 6630–6634.

16 L. Zhong, J. Xiao, Y. Lu, Y. Guo and D. Kong, US Patent 8293963, 2012.

17 J. Huang, X. Han, S. Yang, T. Cao, C. Yuan, Y. Liu, J. Wang and Y. Cui., *J. Am. Chem. Soc.*, 2019, **141**, 8996–9003.

18 T. Mitra, K. E. Jelfs, M. Schmidtmann, A. Ahmed, S. Y. Chong, D. J. Adams and A. I. Cooper, *Nat. Chem.*, 2013, **5**, 276–281.

19 B. Moulton and M. J. Zaworotko, *Chem. Rev.*, 2001, **101**, 1629–1658.

20 B. Gao, L.-L. Tan, N. Song, K. Li and Y.-W. Yang, *Chem. Commun.*, 2016, **52**, 5804.

21 M. Wang, J. Zhou, E. Li, Y. Zhou, Q. Li and F. Huang, *J. Am. Chem. Soc.*, 2019, **141**, 17102–17106.

22 Y. Zhou, K. Jie, R. Zhao and F. Huang, *J. Am. Chem. Soc.*, 2019, **141**, 11847–11851.

23 B. Moosa, L. O. Alimi, A. Shkurenko, A. Fakim, P. M. Bhatt, G. Zhang, M. Eddaoudi and N. M. Khashab, *Angew. Chem., Int. Ed.*, 2020, **59**, 21367.

24 A. Chaix, G. Mouchaham, A. Shkurenko, P. Hoang, B. Moosa, P. M. Bhatt, K. Adil, K. N. Salama, M. Eddaoudi and N. M. Khashab, *J. Am. Chem. Soc.*, 2018, **140**, 14571–14575.

25 A. Dey, S. Chand, L. O. Alimi, M. Ghosh, L. Cavallo and N. M. Khashab, *J. Am. Chem. Soc.*, 2020, **142**(37), 15823–15829.

26 A. Dey, S. Chand, B. Maity, P. M. Bhatt, M. Ghosh, L. Cavallo, M. Eddaoudi and N. M. Khashab, *J. Am. Chem. Soc.*, 2021, **143**, 4090–4094.

27 A. L. Spek, Single-crystal Structure Validation with the Program PLATON, *J. Appl. Crystallogr.*, 2003, **36**, 7–13.

28 G. M. Sheldrick, Crystal Structure Refinement with SHELXL, *Acta Crystallogr., Sect. C: Struct. Chem.*, 2015, **71**, 3–8.

29 P.-Q. Liao, N.-Y. Huang, W.-X. Zhang, J.-P. Zhang and X.-M. Chen, *Science*, 2017, **356**, 1193.

30 Z. Zhang, Q. Yang, X. Cui, L. Yang, Z. Bao, Q. Ren and H. Xing, *Angew. Chem., Int. Ed.*, 2017, **56**, 16282.